

A Study of Eddy currents in a Linear Induction Furnace Using Finite Element Method

Adil H. Ahmad*, Akram F. Batti**, Essam M. Abdul-Baki***

Received on: 14/9/2004

Accepted on: 18/7/2005

Abstract

This paper is concerned with a deep study of the magnetic field intensity distribution and the induced eddy currents in a core (the work piece) of a linear induction furnace. Numerical technique is considered in this study based on a general-purpose finite element package "ANSYS 5.4".

The magnitude and direction of the current density of the induced eddy current in each point inside and at the external surfaces of the core of the induction furnace are well analyzed and determined. The effect of a wide range of frequencies on the magnetic field intensity distribution through the core are investigated and presented.

Magnetic and non-magnetic isotropic linear materials are considered as a core for furnaces with rotational symmetry. The achieved results show a good agreement and accuracy with respect to the previous work in this field. Therefore, the package represents an efficient tool to study the effect of furnace geometry, voltage, and frequency of the power supply on the core of the furnace.

Key word: Induction Furnace, Finite Element Method, ANSYS, Eddy currents, Numerical Analysis.

دراسة عن التيارات الدوامة في الأفران الحثية الخطية باستخدام طريقة العنصر المحدد

خلاصه

هذه الورقة معنية بدراسة عميقة عن توزيع المجال المغناطيسي و التيارات المحتثة في القلب (العينة) لفرن حثي خطي. اعتمدت التحليلات الرقمية في هذه الدراسة وذلك باستخدام برمجيات متعددة الاستخدامات "ANSYS 5.4" لطريقة العنصر المحدد.

لقد تم تحليل و تحديد مقدار واتجاه كثافة التيارات المحتثة في كل نقطة داخل القلب وعلى سطوحه الخارجية بصورة جيدة. كما تم استقصاء وتوضيح تأثير مدى واسع من الترددات على توزيع شدة المجال المغناطيسي.

تم الأخذ بنظر الاعتبار مواد مغناطيسية ولا مغناطيسية من النوع المتساوية الخصائص في جميع الاتجاهات كقلب لأفران ذات تماثل دوراني و أظهرت النتائج التي تم الحصول عليها دقة و انسجاما جيدا مع أبحاث سابقه في هذا المجال. لذلك تمثل هذه البرمجيات أداة كفاه لدراسة تأثير شكل الفرن، وفولتية و تردد مجهز ألفدره على قلب الفرن.

List of Symbols:

$| |$: Absolute value of a vector

quantity.

$[]$: Matrix.

$\{ \}$: Column vector.

$\nabla \times$: Curl of a vector.

$\nabla \cdot$: Divergence of a vector.

∇ : Gradient of a scalar.

A : Magnetic vector potential Wb/m

B : Magnetic flux density Tesla.

* Elect. Eng. Dept. UOT

** Technical Education Dept., UOT

*** Al-Rasheed College/Elec. Eng. UOT

- D : Electric flux density Amp.s.m^{-2} .
 E : Electric Field intensity V.m^{-1} .
 H : Magnetic field intensity Amp.m^{-1} .
 I : Current Amp.
 J : Current density Amp.m^{-2} .
 V : Electric scalar potential V.
 μ : The permeability Henry.m^{-1} μ_r :
 The relative permeability.
 ν : The reluctivity A.m.Wb^{-1} .
 ρ : The resistivity $\Omega.m$.
 σ : The conductivity ($\Omega.m$)⁻¹

Introduction

The induction furnace is simply an A.C. fed coil; its core is heated due to the induced eddy currents produced through it. The induction heating is one of the most important industrial processes, that is a clean and economic method in heat treatment of materials.

The old design of such a furnace depends on experience associated with an approximated circuit analysis^[1]. Such a type of design will be expensive and consumes a lot of time to be finished, while nowadays the new studies avoid such limits by the aid of numerical analysis methods. These are used to solve the partial differential equations of such complicated and multidiscipline system, which is done in this research.

This work presents the application of Finite Element Method (FEM) for the numerical analysis of linear induction devices with rotational symmetry. Two types of furnace cores are analyzed and simulated. The core of the first furnace is a nonmagnetic conducting medium with rotational symmetry and a constant scalar conductivity and permeability ($\mu_r=1$). The second core is a magnetic conducting medium with rotational symmetry and a constant

scalar conductivity and permeability ($\mu_r=200$). The external sources are stationary coaxial coils, which carry time-harmonic azimuthally constant currents. The steady-state analysis of this problem leads to linear elliptic partial differential equations with discontinuous coefficients. Analytical solution is possible only if the medium has additional symmetry, e.g., spherical or infinitely long circular cylindrical conductor. In all other cases, numerical treatment is required. Hence, a general-purpose finite elements package "ANSYS 5.4" is considered to analyze such a system in order to determine the behavior of the induced eddy currents and their heat losses everywhere inside the core of the furnace. In spite of the assumptions of linearity for such a non-linear system the obtained results will explain what is going on inside and at the surfaces of the core of such a furnace. This gives an investigation about the generated eddy currents and their relations with the supplied current to the furnace and the effect of furnace geometry on its distribution.

Finite Element Method

The finite elements method is a numerical method which provides an approximate solution of the boundary valued problems where the phenomena are described by a set of partial differential equations for which there is no visible analytical solution. It derives its name from the basic concept of the method, which involves the subdivision of the domain under consideration into a number of small regions called elements. The elements can have different shapes and can be put together to model any irregular and

complex objects composed of different materials and have mixed boundary conditions. Inside each element the variation of the unknown field value can be approximated by a piecewise trial polynomial function, this function is known as the shape function varies from linear to up to eighth order (for a 2-D case) depending on the number of nodes that forms the element^[2]. The degree of accuracy of the solution depends on both the number of elements describing the object, and the degree of approximation of the field variation inside the element (number of nodes describing an element). The usual element type in the 2-D electromagnetic modeling is the three nodes linear triangular element, or the eight nodes higher order quadrilateral element^[3].

Having got a partial differential equation, the process of formulation by the finite elements method through the following steps: -

- i. Select a paper type of shape function, i.e. the element type.
- ii. Work for finding the expression of the element matrix in terms of the nodal dimensions, the material and the load vector. The derivation of the element matrix of the electromagnetic problem can be either based on minimizing the energy functional of the hall domain (the variational approach) or minimizing the weighted integral of the residual in an element domain (the Galerkin Weighted Residual Approach) in which the function is taken to be the shape function. Details of the element matrix derivation by the two approaches can be found in many literatures^[2-6]

iii. The element matrices are assembled into the global matrix and after the substitution of the known boundary condition nodal values, a set of simultaneous equations of the following general form is obtained.

$$[K]\{A\} = \{f\} \dots\dots\dots (1)$$

where [K] is called the stiffness matrix, it is symmetric and sparse ; {A} is the nodal unknown vector (or the Degree Of Freedom, DOF) and {f} is the load vector. Solution to the above equation can be obtained by various matrix techniques, Gaussian elimination, Gauss –Siedal etc. More recently, however, the Preconditional Conjugate Gradient method and the Frontal Solver have been found to be efficient in handling large sparse systems and are now popularly used.

For an electromagnetic device, basically, the field is generated by the current or by the permanent magnet. In most cases current flows either in a solid conductor or in a stranded coil, a stranded coil consists, usually, of isolated turns of thin conductor, in which eddy currents are not considered.

The usual static formulation of an element matrix starts from Maxwell's equations,

$$\nabla \times \{H\} = \{J\} + \{\partial D / \partial t\} \dots\dots\dots (2)$$

Neglecting the displacement current for low frequencies leads to

$$\nabla \times \{H\} = \{J\} \dots\dots\dots (3)$$

And

$$\nabla \times \{E\} = -\{\partial B / \partial t\} \dots\dots\dots (4)$$

$$\nabla \cdot \{B\} = 0 \dots\dots\dots (5)$$

Finite elements analysts of electromagnetic devices usually build their models considering the excitation coils as current density region that follows the well known Maxwell's equations.

The constitutive relations that describe the behavior of the electromagnetic material are

$$\{B\} = [\mu]\{H\} \dots\dots\dots (6)$$

$$\{J\} = [\sigma]\{E\} \dots\dots\dots (7)$$

The relation defines using the vector identity with equation (5), the magnetic vector potential A

$$\{B\} = \nabla \times \{A\} \dots\dots\dots (8)$$

$$\{E\} = -\{\partial A / \partial t\} - \nabla V \dots\dots\dots (9)$$

$\{A\}$ = Magnetic vector, of potential vector.

V = Electric scalar potential

These specifications ensure the satisfactions of two of Maxwell's equations (3) and (5), what remains to be solved in Ampere's law.

For simplicity differential equations for the system are^[3]:

$$\nabla \times [\nu] \nabla \times \{A\} + [\sigma] \{\partial A / \partial t\} + [\sigma] \Delta V = \{0\} \dots\dots\dots (10)$$

where the last two terms correspond to the two current density components namely eddy and source respectively. Another differential equation is that which describes the core region as

$$\nabla \times [\nu] \nabla \times \{A\} = -[\sigma] \{\partial A / \partial t\} \dots\dots\dots (11)$$

These two equation models the conducting region in the whole domain while for non-conducting region the differential equation is:

$$\nabla \times [\nu] \nabla \times \{A\} = \{0\} \dots\dots\dots (12)$$

while that which describes the coil region is

$$\nabla \times [\nu] \nabla \times \{A\} = -[\sigma] \nabla V = -J^s \dots\dots\dots (13)$$

where $\{J^s\}$ is the source current density vector, $[\sigma]$ is the conductivity matrix, and $[\nu]$ is the reluctivity matrix $= [\mu]^{-1}$. Equation (13) is reduced for the static isotropic two dimensional problem to the well known Poisson's equation, where A_z is the only component of the magnetic vector potential, and J has only the in-plane component.

$$\nu(\partial^2 A_z / \partial x^2) + \nu(\partial^2 A_z / \partial y^2) = -J^s \dots\dots\dots (14)$$

When neglecting the velocity effect, the application of the finite element procedures of equation (13) and equation (14) leads to the element matrix of the form^[5]

$$\begin{bmatrix} [C^{AA}] & [C^{Av}] \\ [C^{Av}] & [C^{vv}] \end{bmatrix} A_{ze} + \begin{bmatrix} [K^{AA}] & [0] \\ [K^{Av}] & [0] \end{bmatrix} A_{ze} = \begin{Bmatrix} \{J^s\} \\ \{I^s\} \end{Bmatrix} \dots\dots (15)$$

This element matrix represents a set of partial differential equation in which nodal element magnetic vector potential A_{ze} is unknown (DOFs),

$\{J^s\}$ is the source current density vector for the element and $\{J^t\}$ is the total current density vector for the element and can be assumed as uniformly distributed current density owing to the impressed current in solid conductor. Assembling all element matrices and applying the boundary conditions on nodes will leads to the solution in the whole domain. Details of the coefficient matrices derivation are given in reference [5].

Induction Furnace with Non-Magnetic Core:

The first analysis is done using a published data in references [6 & 7] for a non-magnetic core induction furnace in order to verify the present work. The data are presented in Table -1- for a cylindrical specimen of a conducting material, the cross-section of the furnace is shown in Fig.-1-.

Table (1)
Coil and Load Data

Coil radius r_2 (m)	0.16
Coil length L (m)	0.32
Supply frequency	Variable
Load radius r_w (m)	0.1
Load length L (m)	0.32
Conductivity (mho/m)	3.4×10^7

The rotational symmetry is very clear, so axisymmetric model is considered in this study. Two frequencies are considered (4.47 Hz and 31Hz) in solving the model, the coil is considered as "a constant current fed stranded coil", supplied with a current density ($J^s = 2 \times 10^6 \text{ A.m}^{-2}$). The results show a good agreement with that obtained by using Boundary Integral

Equation (BIE)^[7] and that by using Hybrid Method (Finite Element Method together with Boundary Elements Method)(FEM-BEM)^[8] as shown in Fig. (2-a, b). The results represent the normalized tangential component of magnetic intensity to the charge mid-plane surface values ($\frac{H_t}{H_t(r_w, L/2)}$), it shows similar profile to that given in both references [7 & 8].

Induction Furnace with Magnetic Core:

To fulfill the aim of this research an induction heating coil having a steel core of cylindrical form, with following parameters ($\mu_r = 200$, $\rho = 0.184 \times 10^{-6} \Omega.m$ at 0°C).

The coil is considered as a stranded coil fed by constant current density $J^s = 2 \times 10^6 \text{ Am}^{-2}$ with different frequencies (50, 500, 1K, 5K) Hz. The results show the distribution of the magnetic intensity, flux lines and current density everywhere inside and on the surfaces of the core. Evaluation of H and J in magnitude and direction is shown graphically. A contour plot is obtained to show the heat distribution inside the core as a measure of the power losses due to the generated eddy currents.

Simulation Results:

The F.E.M. package "ANSYS 5.4" shows the flux path inside and outside the furnace at one instant depending on the phase of supply current to the furnace coil, so

Fig. (3) shows a longitudinal section of the furnace and its boundary region as a circle of a radius nearly three times as that of the furnace, the flux

lines generated at seven instants show a time for quarter cycle of the supply current, starting from Fig. (3-a) at angle=0° (corresponding to time $t=0$ sec.) when the supply current is in its maximum value and Fig. (3-b) shows the distribution at angle=15°, and so on up to Fig. (3-g) which show the distribution at angle = 90° (corresponding to time $t = T/4$ sec., $T=1/f$) which represents the flux lines when the instantaneous supply current = 0 Ampere at this instant. Fig. (3) is drawn for a supply current of 50Hz for the magnetic core described above. The results show that the flux density is not the same at all parts of the core.

To evaluate the magnitude of H inside the core, certain levels are chosen and $|H|$ is drawn as a function of core radius for different levels as shown in Fig. (4). This graph is given for 50Hz supply current; it shows that the core center will have the higher intensity near the surface and it is reduced towards the top surface of the core. Fig. (5-a) shows the vector representation of H at five levels inside the core at time $t=0$ sec. This figure shows possible directions of H in the (X-Y) plane, and its magnitude is position dependent, the higher magnitude is at the surface of the level (a-b) at the center of the core. Other components disappear due to their low values. Fig. (5-b) shows only the direction of all H components. The magnitude and direction of B are not considered because of the linearity assumption of the

magnetic circuit and therefore $B = \mu H$ always.

The current density J displayed in five layers as shown in Fig. (6) as a vector plot, this result show that the highest component is on the surface of the layer at the center and this component reduced gradually up to the top surface layer.

The results in figures 5 and 6 show the magnitude and direction for H and J at ($t=0$). If each vector of any element followed at a time step for a period of one cycle it will show a complete sinusoidal waveform at the same frequency as that of the source current, but with different lagging phase angle at each element of the model.

To study the effect of different frequencies on the operation of the induction furnace Fig. 7 show the normalized magnitude of H as a function of radius of the specimen at the center level (a-b) for the frequencies (50,500,1K, & 5K) Hz. This figure show the Skin effect clearly, and it show a good agreement with the results obtained by references [7 & 8]. Fig. (8) shows normalized $|H|$ distribution of these frequencies on the boundary (the path jb in fig. (1-b)), and it shows an expected reasonable result agreed with the published results [7&8].

Conclusion:

The simulated results obtained show the validity of the Finite Element Computer package (ANSYS 5.4) in analyzing the induction heating coils due to the following properties which provide a suitable tool and make it easy for the researcher to imagine the induction process easily: -

1. Obtaining the optimum meshing size and distribution for the finite elements in the model to be studied in order to achieve the most accurate result with shortest processing time.
2. Specifying the magnetic field quantities (B, H, J) in both space and time domain by drawing a vector plot for nodal results and element results for the quantities at any instant and at any selected path in the model. This will lead to declare their imagination and behavior in such domains.
3. Calculation of the real and imaginary components of the above parameters, which will make it easy to obtain the peak and the r.m.s. Values easily.
4. Ability to show a contour plot mapping for flux path and other scalar quantities like power and joule heat distribution anywhere inside the model.

The achievement of this work, in spite of the agreement of the obtained results with that already published^[7,8], is its ability to show the behavior of H , and J in time domain (by calculating each component in different instants).

The time domain analysis shows sinusoidal variation of these quantities as follows:

a. The quantities B & H

Each one has a pulsating component in $\pm X$ & $\pm Y$ directions in each element which varies in sinusoidal waveform with time, and at frequency (f) (where "f" is the frequency of the supply current of the furnace coil) but with different lagging phase angle each, so the resultant value for B or H may take any direction in the (X-Y) plane at any instant. The results in Fig. (6-a) show that the distribution of H is not uniform inside the core, and

the highest concentration occurs at the center of the core behind the surface. Fig. (7) shows that this distribution as a function of the supplied frequency (with constant current density) which show the Skin effect. The expected results for B are the same as that of H since $B = \mu H$.

b. The current density J

The current density J of each element has a pulsating component in $\pm Z$ direction and this component varies in sinusoidal waveform with time at the same frequency (f) of the supply current but with different lagging phase angle each. This result leads to the conclusion that each element at the specimen section will conduct a current in a short circuited tube of conductor around the specimen with a radius which depends on the position of the element in this section and with cross-sectional area equal to that of the element. Hence, if we assume the element current to be I_e and the element area as A_e and the element current density J_e then

$$I_e = |J_e| \cdot A_e \dots\dots\dots (16)$$

and

$$R_e = \rho(I_e / A_e) \dots\dots\dots (17)$$

where $l_e = 2 \times \pi \times r_e$, and r_e is the distance between the specimen center line and the element center. Hence, the power losses of that tube of current is

$$P_e = (I_e)_{rms}^2 \times R_e \dots\dots\dots (18)$$

The total power losses will be the summation of the power loss in each elementary tube of current in the core

(or specimen). The elementary tube currents are really, what is known as "eddy currents", and the results show that these currents are of different magnitudes and lagging angles with respect to the excitation current (the source current). So the magnitude and phase angle of each current depend on the position of its path, the frequency used, and the material parameters. From the previous discussion and by knowing the other capabilities of ANSYS package the researchers may study the effect of the non-linearity in the magnetization characteristics (The B-H curve) on this process. Also by using the coupling facility between different disciplines a study of the "Thermal Analysis" of the furnace can be done in order to achieve a complete simulation, but this will lead to take the effect of the non-linear dependence of the resistivity ρ and the relative permeability μ_r with the temperature of the furnace. By taking all of these non-linear ties into consideration the simulation will be as true as possible to reality. Such a study will show a real numerical computer aided induction furnace design, which will aid the designers to build-up, an efficient and economic induction heater.

References

1. Davies, J. and Simpson, P., Induction Heating Handbook,

McGraw-Hill Book Company (UK), 1979.

2. M.V.K. Chari and P. Silvester, "Finite Element Analysis of Magnetically-Saturated D.C. Machines", IEEE Trans, PAS-90, pp. 2362-2368, 1971.
3. Hong Cheng Lai, Coupling Finite Element Meshes for Modeling Movement in Electromagnetic Devices, Ph.D. Thesis, University of Bath UK, 1994.
4. M.V.K. Chari and P. Silvester, Finite Element in Electrical and Magnetic Field Problems, John Wiley & sons (1980).
5. S. Rao, The Finite Element Method in Engineering, Pergamon Press, (1982).
6. Biro, Oszkar and Preis, Kurt, "On The Use of Magnetic Vector Potential In The Finite Element Analysis of Three-Dimensional Eddy Currents", IEEE Trans. On Magnetics, Vol. 25, No.4, (1989).
7. T. H. Fawzi, K. F. Ali, and P. Earl Bruk, "Boundary Integral Equations Analysis of Induction Devices with Rotational Symmetry", IEEE Trans. On Magnetics, Vol. MAG.19, No.1., pp. 36-44, Jan. (1983),
8. Razzaq A. Marsuq, Analysis and Study of Design Criteria of Induction Furnaces, M.Sc. Thesis University of Baghdad ad, (1994).

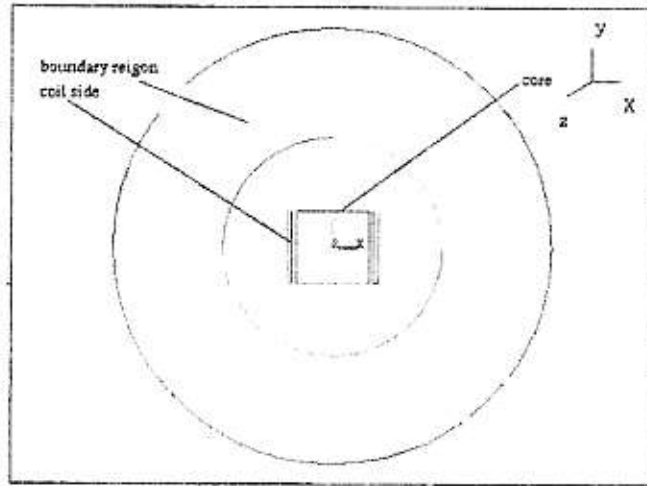


Fig. (1-a)
A cross-section in the furnace with the boundary region

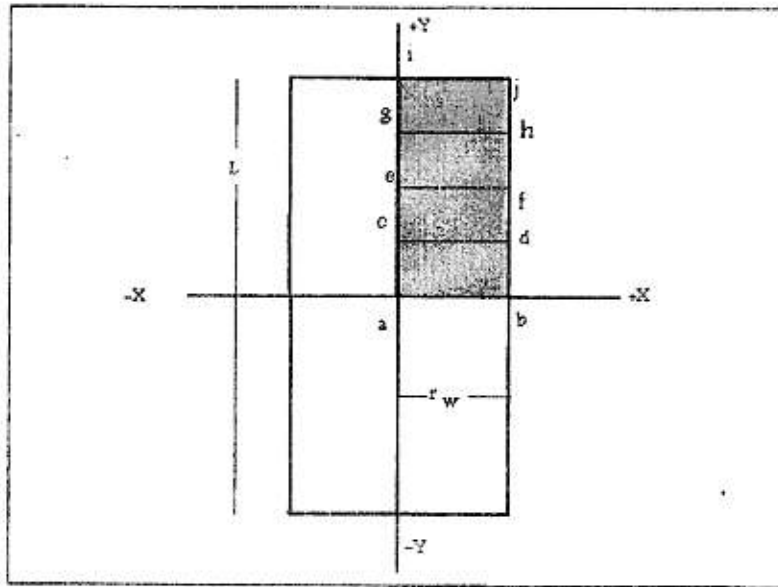
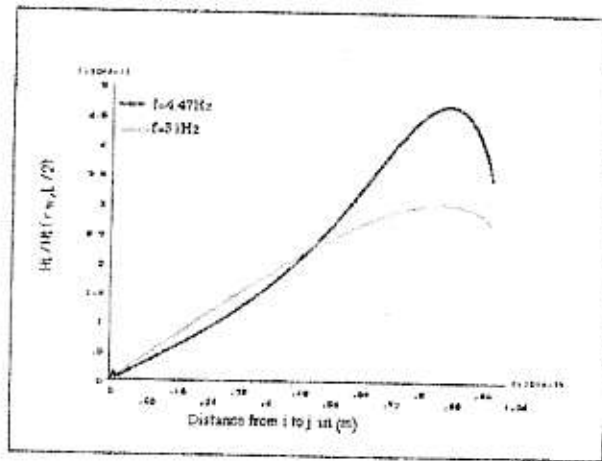
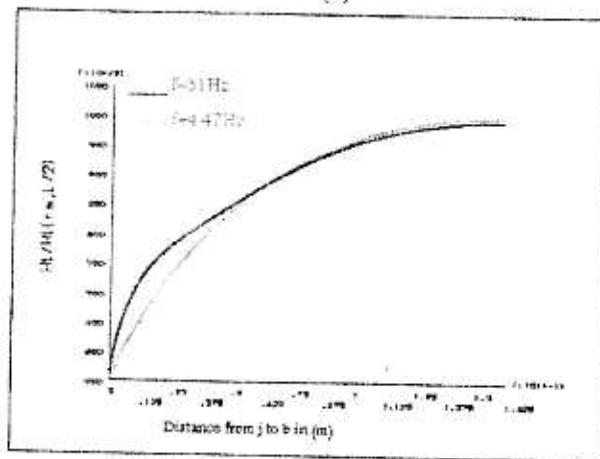


Fig. (1-b)
A longitudinal-section in the core of the furnace shows the symmetry. The area (abji) in the first quarter is considered in the analysis. The lines (a-b), (c-d), (e-f), (g-h), & (i-j) are the five levels used for extracting the results.



(a)



(b)

Fig. (2) The normalized tangential component of magnetic intensity at 4.47Hz and 31Hz supply frequencies for the cases
(a) Along the distance i to j.
(b) Along the distance j to b.

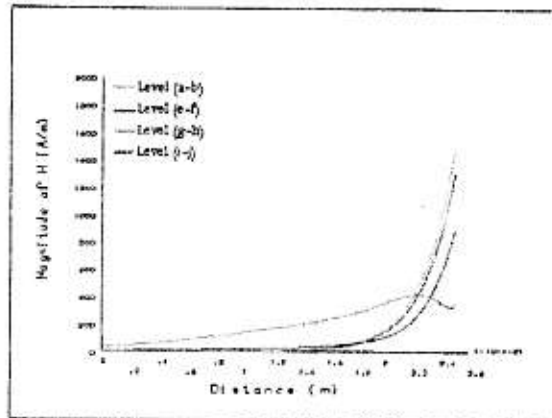


Fig. (4) Distribution of $|H|$ with core radius for different levels inside the core.

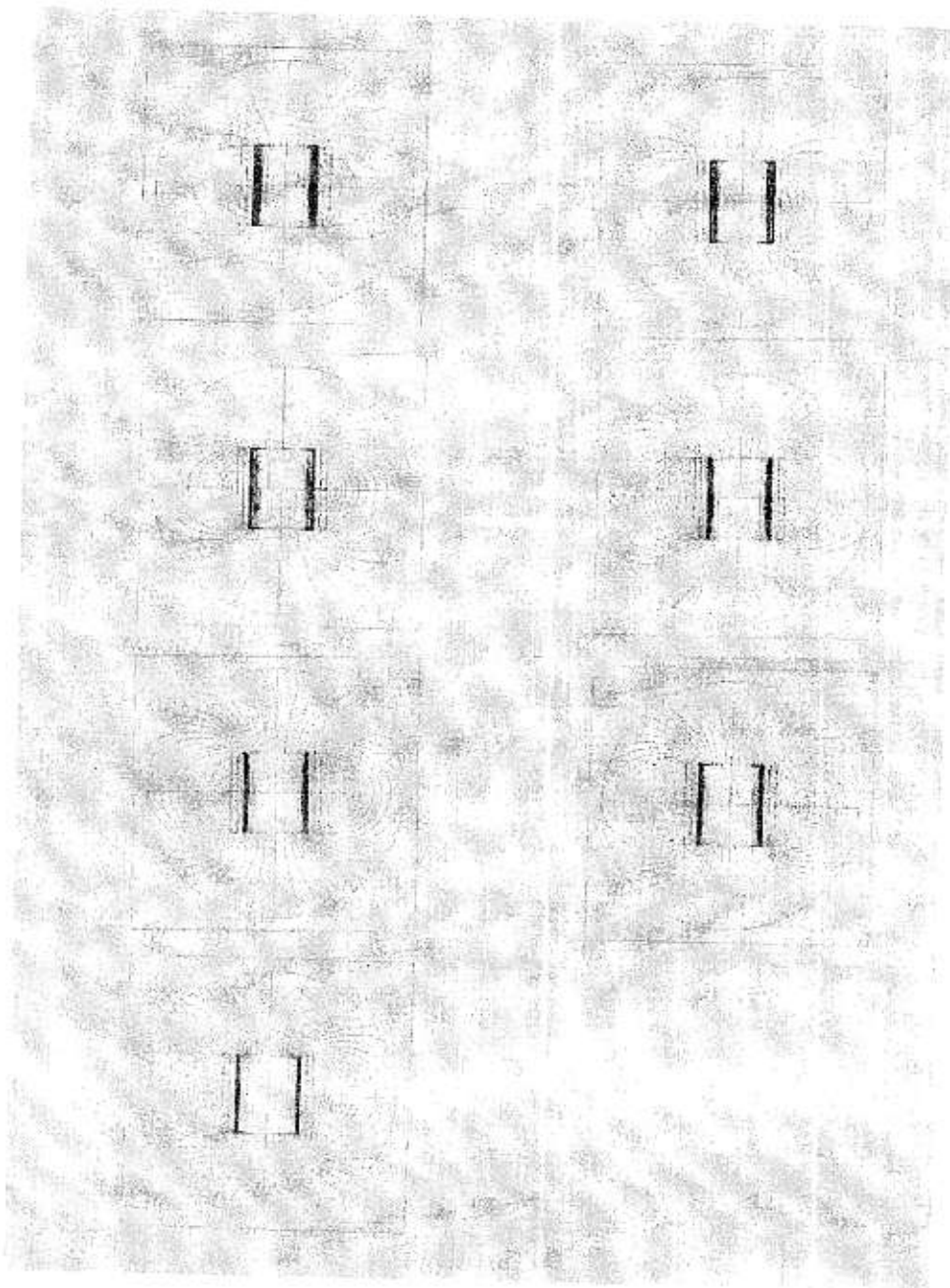
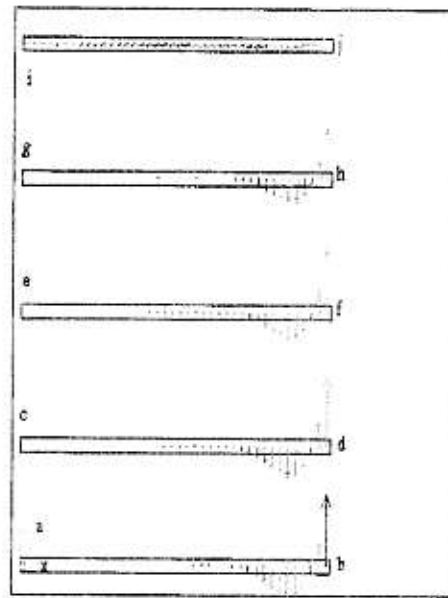
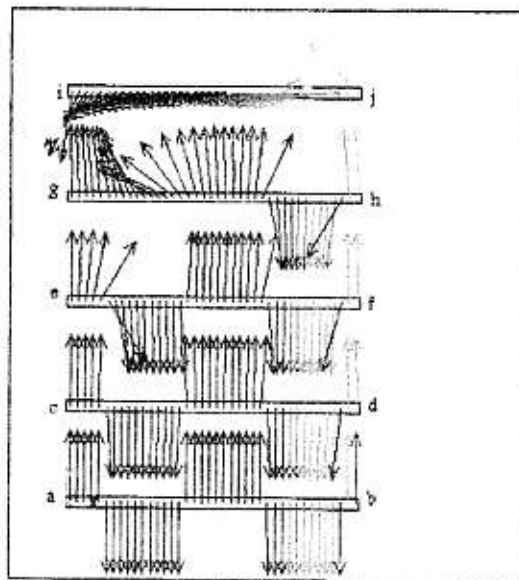


Fig. (3) Flux distribution during a quarter cycle of the supply current at angles
($a = 0^\circ$, $b = 15^\circ$, $c = 30^\circ$, $d = 45^\circ$, $e = 60^\circ$, $f = 75^\circ$, $g = 90^\circ$)



(a)



(b)

Fig. (5) Vector representation of H in five levels inside the core show the possible magnitude and direction of this vector quantity at 50Hz case.

- (a) Magnitude based.
- (b) Uniform magnitude.

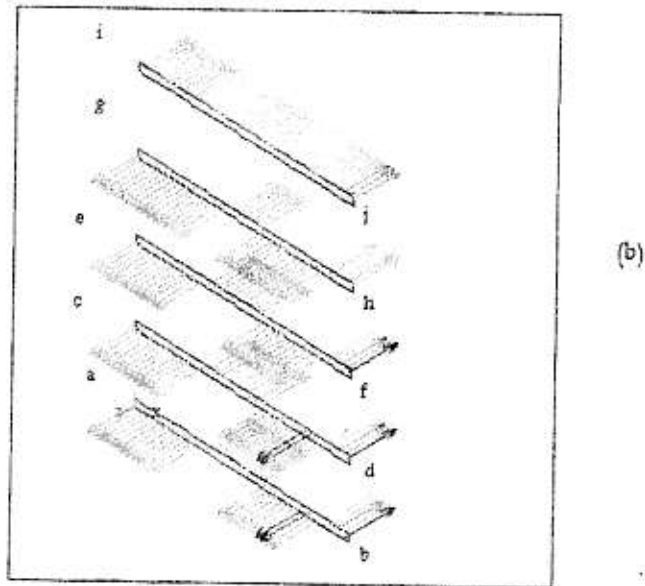
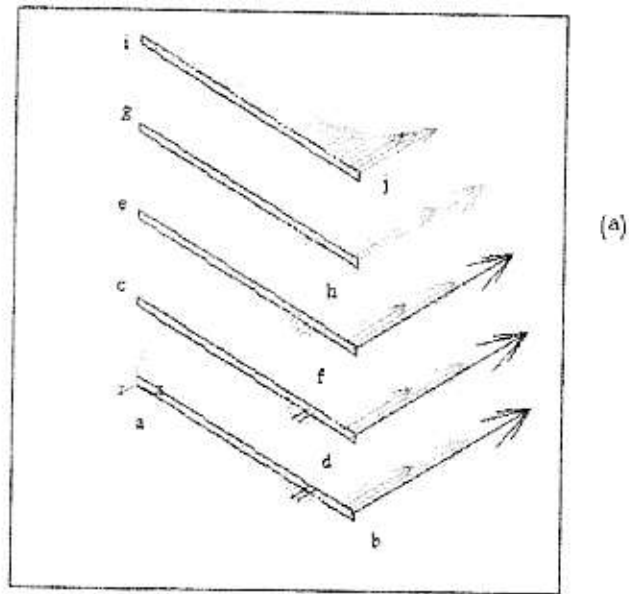


Fig. (6) shows the current density components in the five layers
(a) Magnitude based (b) Uniform magnitude.

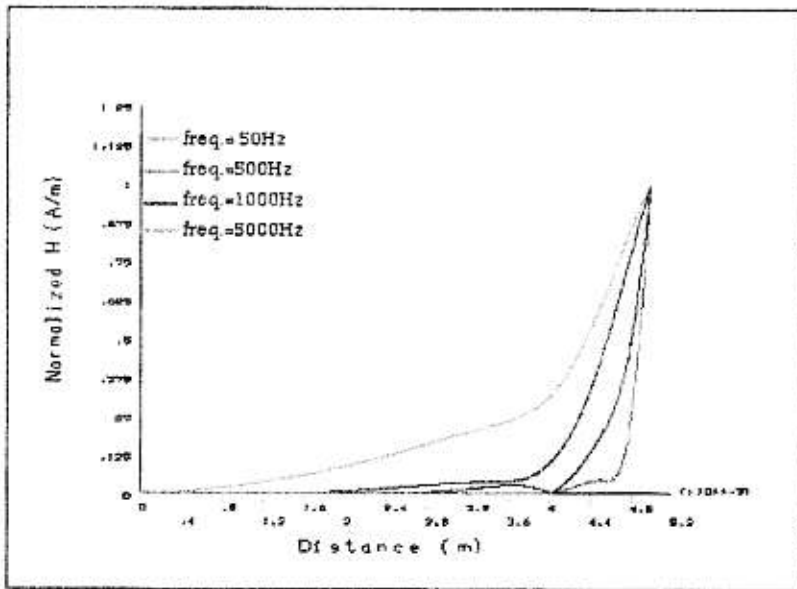


Fig. (7)

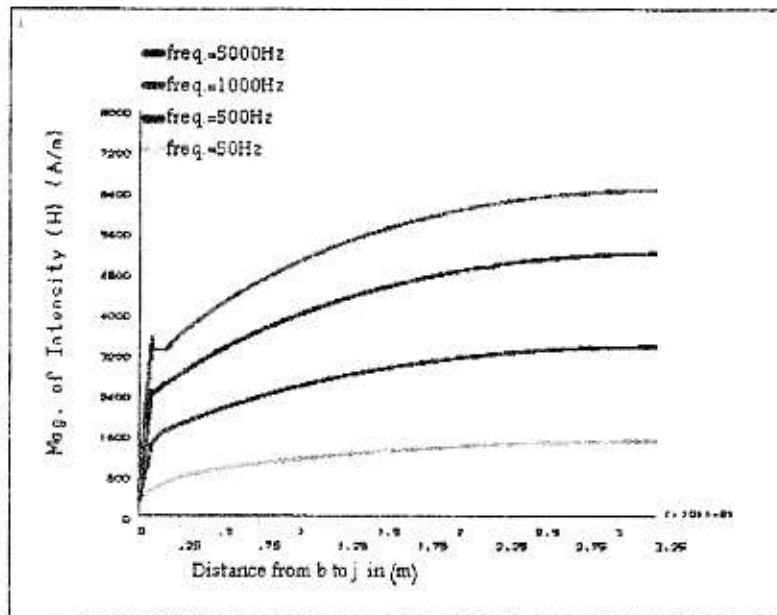


Fig. (8) Distribution of $|H|$ for different frequencies